ISSN: 2093-5374 / E-ISSN: 2093-5382

Optimized FBMC-OQAM-CDMA Framework for Low-Complexity Interference Mitigation in MIMO Systems with Space-Time Coding

Satish Kanapala[1*], and Shaik Jakeer Hussain[2]

[1*]Assistant Professor, Department of Electronics and Communication Engineering, Vignan's Foundation for Science, Technology and Research, Guntur, India. satishkanapala@gmail.com, https://orcid.org/0000-0002-7728-4035

[2]Professor, Department of Electronics and Communication Engineering, Vignan's Foundation for Science, Technology and Research, Guntur, India. jk.shaik@gmail.com, https://orcid.org/0000-0002-4538-7451

Received: September 22, 2025; Revised: November 15, 2025; Accepted: December 17, 2025; Published: March 31, 2026

Abstract

The evolution of Multiple Input Multiple Output (MIMO) technology has significantly strengthened wireless communication performance; however, persistent challenges remain in interference mitigation, computational complexity, and spectrum efficiency. Filter Bank Multicarrier with Offset Quadrature Amplitude Modulation (FBMC-OQAM) has emerged as a viable alternative to Orthogonal Frequency Division Multiplexing (OFDM). This non-orthogonal waveform is attractive because of its low out-of-band radiation and high spectral efficiency. Nevertheless, inter-symbol and inter-carrier interference arising from the non-orthogonal nature of FBMC-OQAM signals and computational complexity degrade system performance. To address these challenges, this paper will present a new framework which is a synergistic integration of Code Division Multiple Access (CDMA), FBMC-OQAM, and space-time coding in MIMO. There are three major goals of the suggested strategy. To reduce mitigation of interference, the incorporation of CDMA spreading sequences is done to reduce inter-symbol and inter-carrier interference. Second, the space-time coding is designed with the aim of minimizing the number of computations made without affecting the performance. Third, the framework's objective is to improve bit error rate and other performance indicators, spectral efficiency, and robustness against multipath fading, ensuring reliable communication in MIMO environments. Performance of the proposed method is assessed and contrasted with additional benchmark models. Experimental results show that integrating CDMA with FBMA-OQAM and space-time coding significantly reduces interference, minimizes complexity, and enhances spectral utilization. The developments will ensure that future wireless networks can enjoy quality and dependable communication procedures. The proposed work establishes a solid foundation for the practical implementation of FBMC-OQAM in MIMO systems.

Keywords: MIMO, FBMC-OQAM, Spectral Efficiency, Space Time Coding, Zero-Forcing, Maximum Likelihood.

Journal of Wireless Mobile Networks, Ubiquitous Computing, and Dependable Applications (JoWUA), volume: 17, number: 1 (March - 2026), pp. 120-141. DOI: *10.58346/JOWUA.2026.I1.008*

*Corresponding author: Assistant Professor, Department of Electronics and Communication Engineering, Vignan's Foundation for Science, Technology and Research, Guntur, India.

1 Introduction

Future wireless communication systems, such as massive machine-type communications (match), ultra-reliable low-latency communications (URLLC), and enhanced mobile broadband (ebb), must evolve to meet the requirements of emerging network scenarios (Popovski et al., 2018; Walia et al., 2025; Tandon & Thakur, 2025; De Almeida et al., 2019). As these networks are expected to define the future of telecommunications, they must satisfy specific requirements (Säily et al., 2020; Lenine et al., 2025). Therefore, the waveform for the next-generation wireless networks must be designed to meet these demands. Currently, Orthogonal Frequency-Division Multiplexing (OFDM) is widely used in wireless networks due to its effectiveness in frequency-selective channels. However, OFDM has drawbacks. It employs a rectangular pulse, which leads to significant issues (Chen et al., 2018), for instance, (i) high out-of-band (OOB) radiation, which interferes with nearby channels; (ii) the Cyclic Prefix (CP) overhead, which reduces spectral efficiency; and (iii) the need for strict time and frequency synchronization to preserve orthogonality. These limitations make OFDM less suitable for all application scenarios. These limitations highlight the need for new waveforms to address the challenges of next-generation networks (ChithraDevi et al., 2024).

To address these challenges, techniques like filtering and windowing have been applied, but remain insufficient. All these limitations of OFDM have driven researchers to explore alternative waveforms that can meet the demands of next-generation communication systems. One prominent alternative is Filter Bank Multicarrier with Offset Quadrature Amplitude Modulation (FBMC-OQAM). This waveform has significant advantages over OFDM, making it suitable for future communication systems. FBMC-OQAM transforms complex-valued QAM symbols into real-valued streams, before transmission (Raslan et al., 2022). Localized prototype filters for time and frequency are used to shape each subcarrier. These filters reduce OoB emissions. Additionally, FBMC-OQAM improves spectral efficiency since it does not use CP (Kadhim et al., 2024; Sahin et al., 2013).

Despite its benefits, FBMC-OQAM suffers from intrinsic interference due to its OQAM constellation (RezazadehReyhani & Farhang-Boroujeny, 2017). This complicates Multiple Input Multiple Output (MIMO) integration. Much research has explored integrating Multiple Input Multiple Output (MIMO) with FBMC-OQAM. In (Caus & Perez-Neira, 2013) Caus and Neira designed precoding and decoding matrices for frequency-selective channels. This approach showed promising outcomes but resulted in Bit Error Rate (BER) floors and increased complexity. Wang et al., (2018) presented a model for interference cancellation in MIMO-FBMC-OQAM using a preamble structure. Compared to conventional methods, this model achieves lower BER. The framework of FBMC developed by Zakaria & Le Ruyet, (2012); Perez-Neira et al., (2016) is quite efficient in eliminating inherent interference through a better design of filters and system setup. The strategy enhances signal orthogonality and robustness of the system. Combined with MIMO architectures, it provides a significant improvement of performance and spectral efficiency. The authors found that the Alamouti technique can only be implemented if CDMA is included (Ghazi et al., 2021). Block-wise Alamouti method was proposed for FBMC employing the PHYDYAS filter (Le et al., 2016). In this configuration, a time-inverted frame structure was employed to encode the transmitted data. Conventional Alamouti decoding could be employed at the receiver to recover data. This straightforward approach preserves the integrity of the FBMC data structure.

Singh et al., (2018) investigated the error rate of MIMO-FBMC-OQAM based on Zero-Forcing (ZF) successive interference cancellation. Nissel et al., (2017) suggested distributing data throughout the time or frequency domain as an effective way to reestablish complex orthogonality in FBMC. This spreading

was efficient as it used the Walsh-Hadamard transform. Their analysis of FBMC-OQAM was conducted using the PHYDYAS prototype filter. In (Arjun et al., 2021), Arjun et al. Designed a low complexity FBMC for MIMO system. The Authors analyzed the effects of interference on various modulation schemes across different signal-to-noise ratio (SNR) levels. The results further indicated that higher-order modulations were affected by interference and were more prominent in high SNR. Bedoui & Et-tolba, (2021) presented a deep neural network for MIMO-FBMC-OQAM interference reduction. This approach showed good results in terms of BER, with increased complexity. In (Varlamov et al., 2023), Varlamov et al. proposed an approach that uses the correlation features of FBMC-OQAM in MIMO systems with memory to perform equalization with self-interference correction. Results showed that the algorithm achieved a comparable level of performance, surpassing the one-tap approach, and it was compared to a more intricate parallel multistage algorithm. The presence of interference causes incompatibility between FBMC-OQAM and MIMO systems. Raslan et al., (2022) presented a block spreading-based effective FBME-OQAM implementation. This spreading restored complex orthogonality to facilitate the use of FBMC-OQAM with MIMO. This method uses the Discrete Haar transform to reduce computational complexity. Performance was evaluated and compared with CP-OFDM and spatial multiplexing with ZF detection. Şimşir, (2024) implemented the Migrating bird's optimization algorithm to reduce interference and complexity in the MIMO-FBMC-OQAM system. Li et al., (2022) used a power multiplexing method to reduce interference in the FBMC-OQAM system. The pulse shaping filters were presented by Abdel-atty (Abdel-Atty et al., 2020) in effort to improve the FBMC-OQAM system performance. The suggested scheme employed the Walsh-Hadamard code in FBMC-OQAM in order to distribute data. The PHYDYAS-based system was more successful. The paper points out that the FBMC-OQAM systems also work in distortion prone channels and therefore it can be a viable alternative in ionospheric communication systems using high frequencies and speeds of communication system. Nonetheless, this system has certain shortcomings such as inter-symbol and inter-carrier interference occasioned by the non-orthogonality of FBMC-OQAM and a heavy computation load when dealing with a multi-antenna space-time coded system. In this paper, the objective is to resolve these problems using the synergies of CDMA and space-time coding in the environment of MIMO. This paper has the following major contributions:

- Suggest a hybrid system combining FBMC-OQAM and CDMA to deal with inter-symbol and inter carrier interference. The suggested approach improves the interference rejection and preserves the benefits of FBMC-OQAM.
- Create a low complexity space time coding and decoding algorithm to work with MIMO systems. This algorithm will minimize complexity in computation.
- Suggest an algorithm to enhance the spectral efficiency of FBMC-OQAM systems in the MIMO systems, such that the frequency spectrum is effectively exploited without reducing the error performance.
- Minimally verify the performance of the proposed framework with multipath fading effect in various propagation conditions, which provides better reliability of MIMO systems.

The remaining part of the paper is as follows: Section 2 describes the FBMC-OQAM in a MIMO setup. The simulation results of the proposed model will be provided in section 3. After Section 4, the paper is concluded.

2 Proposed Model

2.1 Model of the FBMC-OQAM System

Analysing and implementing a MIMO FBMC-OQAM system is the main emphasis of the work. Antennas for both transmitting and receiving signals are part of the system, which allows for better wireless communication. Figure 1 shows the configuration of the proposed system. The system incorporates N_c sub-carriers, which are sufficient for channel delay spread. The transmitter uses a precoder $T(\omega_i)$, and the receiver utilizes an equalizer $R(\omega_i)$ for i=1,2,3… N_c. Here, ω_i refers to the angular frequency of the i^{th} subcarrier. Synthesis Filter Bank (SFB) blocks are located at the transmitter, whereas Analysis Filter Bank (AFB) blocks are located at the receiver (filter bank). Important components of the transmitter and receiver in the proposed MIMO FBMC-OQAM system are $F(\omega)$ and $G(\omega)$. Data is precoded at the transmitter using the matrix $F(\omega)$. This implies that it optimises the usage of the wireless channel and prepares the data to be sent over numerous antennas in a manner that enhances the signal quality. To equalise the received signal, $G(\omega)$ is used on the side of the receiver. It aids in decoupling the mixed signals picked up by various antennas and removing the influence of the wireless channel. Because of this, accurately recovering the original data becomes much simpler. For every subcarrier (frequency) in the system, $F(\omega)$ and $G(\omega)$ operate to ensure that the signal is appropriately handled at that frequency. When used in combination, they boost the wireless communication system's overall efficiency. Using the FBMC-OQAM waveform, we assume that a set of data symbols is sent across N sub-carriers. When broadcast via a p^{th} antenna, the FBMC-OQAM signal is expressed as (Equation 1),

$$S^k[p] = \sum_{m=1}^{N} \sum_{-\infty}^{+\infty} d_{m,n}^k sf_{m,n}[p] \quad (1)$$

Where, $sf_{m,n}[p]$ - at the n^{th} time instant, the synthesis filter associated with the m^{th} subcarrier. It is provided by (Equation 2),

$$sf_{m,n}[p] = s[p - nN/2] e^{j\frac{2\pi m}{N}\left(p - \frac{Lg-1}{2}\right)} e^{j\phi_{m,n}} \quad (2)$$

Where, S[k] - a prototype filter of length L_g and $e^{j\phi_{m,n}}$ - phase term (Renfors et al., 2017). Let $H_m^{(p1,q1)}$ the channel's frequency response between the $p1^{th}$ shown and $q1^{th}$ receive antennas. A common method to represent the signal received at the $q1^{th}$ antenna is as (Equation 3),

$$r^{q1}[k] = \sum_{k=1}^{N_T} \left(\sum_{m=1}^{M} \sum_{n=-\infty}^{\infty} H_m^{(p1,q1)} d_{m,n}^k g_{m,n}[k] \right) + \eta^{(q1)}[k] \quad (3)$$

Where, $\eta^{(q1)}[k]$ represents Gaussian noise. Equation (4) is used to produce the demodulated real symbol corresponding to the m^{th} subcarrier and n^{th} instance.

$$y_{m,n}^{q1} = < r^{q1}[k], g_{m,n}[k] >$$
$$= \sum_{p=1}^{N_T} H_m^{p1,q1} \left(d_{m,n}^{p1} + j u_{m,n}^{p1} \right) + \eta_{m,n}^{q1} \quad (4)$$

Were, $u_{m,n}^{p1}$ – imaginary intrinsic interference. Let the vector containing N_R(Number of Transmit Antennas) demodulated real symbols are denoted as $y_{m,n} = \left[y_{m,n}^1, y_{m,n}^2, \ldots y_{m,n}^{N_R} \right]^T$ and the vector comprising N_T(Number of Transmit Antennas). The transmitted real symbols are represented as $d_{m,n} = \left[d_{m,n}^1, d_{m,n}^2, \ldots d_{m,n}^{N_R} \right]^T$. The demodulation operation in matrix form can then be expressed as (equation 5):

$$y_{m,n} = H_m\left(d_{m,n} + ju_{m,n}\right) + \eta_{m,n} \tag{5}$$

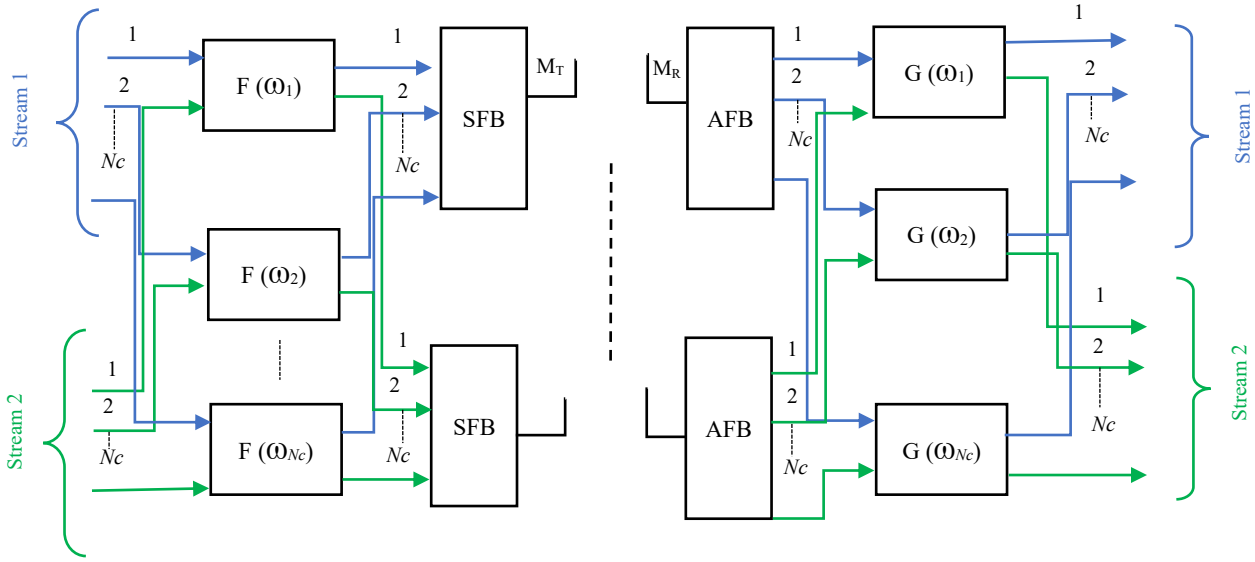

Figure 1: MIMO FBMC-OQAM

Were, H-channel matrix. The signal that was received might be shown as,

$$\begin{bmatrix} y_{m,n}^{1} \\ \vdots \\ y_{m,n}^{N_R} \end{bmatrix} = \begin{bmatrix} H_{m,n}^{11} & \cdots & H_{m,n}^{1N_T} \\ \vdots & \ddots & \vdots \\ H_{m,n}^{N,1} & \cdots & H_{m,n}^{N_T N_R} \end{bmatrix} \begin{bmatrix} d_{m,n}^{1} + ju_{m,n}^{1} \\ \vdots \\ d_{m,n}^{N_T} + ju_{m,n}^{N_T} \end{bmatrix} + \begin{bmatrix} \eta_{m,n}^{1} \\ \vdots \\ \eta_{m,n}^{N_R} \end{bmatrix} \tag{6}$$

2.2 Alamouti Scheme

The Alamouti technique (Alamouti, 2002) may be better understood by looking at the one-tap channel model, as using equation (6),

$$y_k = h_{k,u} s_{k,u} + n_k$$

When the channel gain between the transmit and receive antennas is denoted by $h_{k,u}$ at time instant k, and the additive noise is represented by n_k. We take it as read that $h_{k,u}$ is a unitary-variance Gaussian random process with complex values. Coherent detection is being considered, where the receiver is assumed to have complete knowledge of $h_{k,u}$. Two broadcast antennas and one receive antenna are used to accomplish the Alamouti technique.

In multicarrier modulation, the time and frequency axes may be permuted, so let's use s_{2k} and s_{2k+1} as the two symbols to broadcast at $2k$ and $2k+1$, respectively. Antenna 1 transmits $s_{2k+1}/\sqrt{2}$ at time instant $2k$, whereas antenna 0 transmits $s_{2k}/\sqrt{2}$. Antenna 1 transmits $s_{2k}^{*}/\sqrt{2}$, whereas antenna 0 transmits $-(s_{2k+1})^{*}/\sqrt{2}$. The total transmitted power is normalized by adding the $1/\sqrt{2}$ factor. At time instants $2k$ and $2k+1$, the samples of the received signal are provided by equation (7)

$$y_{2k} = \frac{1}{\sqrt{2}}\left(h_{2k,O}\, s_{2k} + h_{2k,1}(s_{2k+1})^{*}\right) + n_{2k},$$

$$y_{2k+1} = \frac{1}{\sqrt{2}}\left(-h_{2k+1,O}\,(s_{2k+1}) * + h_{2k+1,1}(s_{2k})^{*}\right) + n_{2k+1}, \tag{7}$$

If we assume the channel is constant from $2k$ to $2k+1$ in terms of time, we will get the result as in equation (8),

$$\begin{bmatrix} y_{2k} \\ y_{2k+1}^{*} \end{bmatrix} = \underbrace{\frac{1}{\sqrt{2}} \begin{bmatrix} h_{2k,0} & h_{2k,1} \\ (h_{2k,1})^{*} & -(h_{2k,0})^{*} \end{bmatrix}}_{H_{2k}} \begin{bmatrix} s_{2k} \\ s_{2k+1} \end{bmatrix} + \begin{bmatrix} n_{2k} \\ n_{2k+1}^{*} \end{bmatrix} \quad (8)$$

The transpose conjugate operation is denoted by H, and the identity matrix I_2 has dimensions (2,2), thus $H_2 k H_2^H k = \left(\frac{1}{2}\right)\left(|h_{2k,0}|^2 + |h_{2k,1}|^2\right) I_2$. Keep in mind that H_{2k} is an orthogonal matrix. Hence, the values of s_{2k} and s_{2k+1} are acquired by using the Maximum Ratio Combining (MRC) equalization in equation (9).

$$\begin{bmatrix} \widehat{s_{2k}} \\ \widehat{s_{2k+1}} \end{bmatrix} = \frac{\sqrt{2}}{|h_{2k,0}|^2 + |h_{2k,1}|^2} \begin{bmatrix} h_{2k,0}^{*} & h_{2k,1} \\ (h_{2k,1})^{*} & -(h_{2k,0})^{*} \end{bmatrix} \begin{bmatrix} y_{2k} \\ y_{2k+1} \end{bmatrix} = \begin{bmatrix} s_{2k} \\ s_{2k+1} \end{bmatrix} + \begin{bmatrix} \mu_{2k} \\ \mu_{2k+1} \end{bmatrix} \quad (9)$$

Were,

$$\begin{bmatrix} \mu_{2k} \\ \mu_{2k+1} \end{bmatrix} = \frac{\sqrt{2}}{|h_{2k,0}|^2 + |h_{2k,1}|^2} \begin{bmatrix} h_{2k,0}^{*} & h_{2k,1} \\ (h_{2k,1})^{*} & -(h_{2k,0})^{*} \end{bmatrix} \begin{bmatrix} n_{2k} \\ n_{2k+1} \end{bmatrix} \quad (10)$$

The equation (10) $E(|\mu_{2k}|^2) = E(|\mu_{2k+1}|^2) = 2N_0/(|h_{2k,0}|^2 + |h_{2k,1}|^2)$ holds because the two noise components n_{2k} and n_{2k+1} are uncorrelated. Here, N_0 represents the density of monoliteral noise. Therefore, the bit error probability, abbreviated as p_b, is determined by assuming a QPSK modulation and using the formula from (Tse & Viswanath, 2005) given in equation (11).

$$p_b = Q\left(\sqrt{\left(\frac{|h_{2k,0}|^2 + |h_{2k,1}|^2}{2}\right) SNR_t}\right) \quad (11)$$

Where SNR_t stands for the Signal-to-Noise Ratio on the transmitter side. A diversity gain of 2 will be produced by an uncorrelated pair of channel coefficients.

2.3 CDMA- FBMC-OQAM and Alamouti

In this work, we first review the findings of Lélé et al., (2007) and Lélé et al., (2007) for CDMA-FBMC/OQAM systems, which analyse the transmission of complex and real data symbols, respectively, under the assumption of distortion-free channel conditions. Next, we demonstrate how the proposed system, in combination with Alamouti coding, may be used for transmission across a realistic channel model. We assume that $N_S = M/N_c$ is an integer that indicates the length of the CDMA code by N_c. The u^{th} user's code, represented by $c_u = \left[c_{0,u} \cdots c_{Nc-1,u}\right]^T$, is the transposition operation. For a user u_0 at a certain moment n_0, N_S, various data are sent out as follows: $d_{u0,n0,0}, d_{u0,n0,1}, \ldots, d_{u0,n0,N_s-1}$, when spreading is done in the time domain, such as in pure MC CDMA (Multi-Carrier-CDMA) (Dinan & Jabbari, 2002). Then, at the time n_0 and frequency m_0, we get the actual symbol $a_{m0,n0}$ communicated by spreading with the c_u codes, which is given by equation (12).

$$a_{m_0,n_0} = \sum_{u=0}^{U-1} \frac{c_{m_0}}{N_c}, ud_u, n_0, \left[\frac{m_0}{N_c}\right] \quad (12)$$

The number of users, denoted as U, the modulo operator, and the floor operator are all defined here. The orthogonality of the code ensures that the reconstruction of $d_{u,n_0,p}$ $(where\ p \in [0, N_{S-1}])$ is preserved from the a m_0, n_0 term. Disregarding background noise, the dispersal operator leads to equation (13),

$$\widehat{d_{u,n_0,p}} = \sum_{m=0}^{N_c-1} c_{m,u} a_p N_c + m, n_0 \quad (13)$$

The inclusion of no CP allows for the transmission of these spread real data sets $d_{u,n_0,p}$ to be guaranteed at a symbol rate that is more than double that required for complicated MC-CDMA data transmission, as shown in (Lélé et al., 2010). For real data and a maximum spreading length (defined by the number of subcarriers), the real portion of the symbol is maintained after the dispreading procedure, but the imaginary component $i_{u,n}$ is not identified (see figure 2). A real orthogonality criterion is satisfied by this technique, and it can accommodate up to M users.

The Filter Bank Multicarrier (FBMC) transmission technique employing Offset Quadrature Amplitude Modulation (OQAM) is shown in figure 2. Spectral efficiency is enhanced in this system by the use of well-designed filter banks that retain orthogonality, rather than a Cyclic Prefix (CP). The complex Quadrature Amplitude Modulation (QAM) symbols that make up the input data are first decomposed into their real ($Re\{\}$) and imaginary ($Im\{\}$) parts. The addition of a half-symbol time offset (T/2) to the imaginary components is an essential aspect of OQAM since it guarantees that the real and imaginary portions do not interact with one another and improves the time-domain orthogonality. After this separation, the FBMC waveform is generated by processing the real and delayed imaginary components via a polyphase filter bank. This bank employs the Inverse Discrete Fourier Transform (IDFT) and pulse shaping. When compared to traditional OFDM, this filter bank method enhances frequency localization while reducing spectral leakage. The next step is to time-multiplex the outputs, which means that the transmission of real and imaginary signals happens in alternating time slots. After that, the last signal is transferred via the communication channel, and the receiver uses the inverse procedure to get the initial data. To improve spectrum efficiency and reduce inter-symbol and inter-carrier interference, FBMC employs sophisticated filtering algorithms, in contrast to classical OFDM, which depends on CP for interference mitigation.

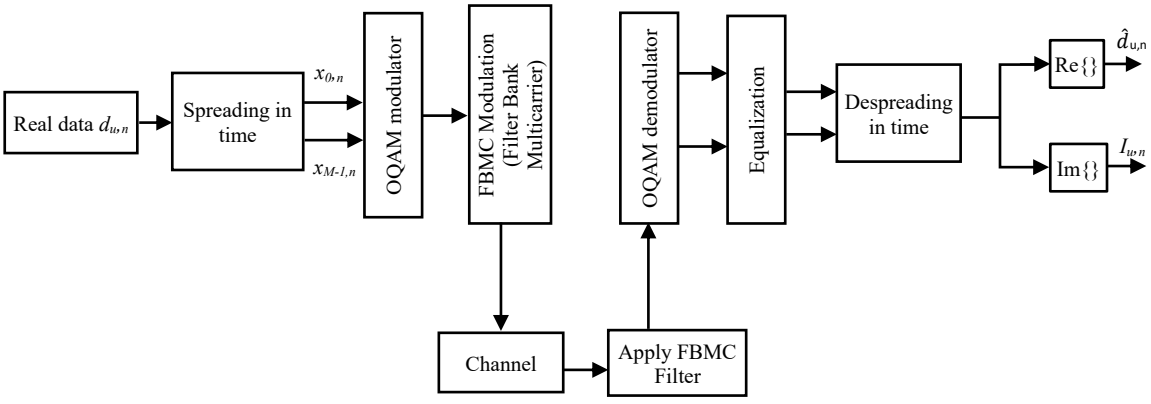

Figure 2: CDMA-FBMC/OQAM transmission scheme

2.3.1 Cancellation of Inferences Process

In (Wang et al., 2010), it is suggested to have a deeper look at the interference term by assuming that the CDMA codes are Walsh-Hadamard (W-H) codes with a length of $M = 2N = 2n$, which is an integer. The length, denoted as $L_g = bM$, of the prototype filter is determined by the indicating function $I_{|n-n0|} < 2b$, which is 1 if $|n - n_0| < 2b$ and 0 otherwise. Once that is done, we can describe the scalar product of the basic functions as in equation (14),

$$\langle g_{m,n}, g_{p,n_0} \rangle = \delta_{m-p,n-n_0} + j\gamma_{m,n}^{p,n_0} \; I\,|n - n_0| < 2b, \tag{14}$$

where $j\gamma_{m,n}^{p,n_0}$ is given below equation (15),

$$j\gamma_{m,n}^{p,n_0} = \zeta\{(-1)^{m(n+n_0)} j^{m+n-p-n_0} A_g(n - n_0, m - p)\} \tag{15}$$

The interference term in the transmission of actual data may be stated in equation (16), according to (Lélé et al., 2007), with a maximum spreading length, $M = 2N = Nc$.

$$i_{u,n} = \sum_{u=0}^{U-1} \sum_{n=-2b+1, n\neq 0}^{2b-1} d_{n+n_0,u} \left(\sum_{p=0}^{2N-1} \sum_{m=0}^{2N-1} c_{p,u_0} c_{m,u} \gamma_{m,n+n_0}^{p,n_o} \right) \tag{16}$$

The cancellation of $i_{u,n}$ interference may be shown in (Lélé et al., 2007) when $U \leq M/2$ spreading codes are appropriately chosen. Given that $M = 2N = 2^n$ is the size of the W-H matrix, it is possible to partition all of the index sets into two sets, S_1^n and S_2^n, where the cardinal is equal to $M/2$. The following is the building rule for these two subsets that ensures users will not interact with each other. When $n = 1$, the first two elements of each subset are initialized to 0 and 1, respectively. Our current assumption is that the two subsets have the following set of indices for an integer $n = n_0$ in equation (17),

$$S_1^{n_0} = \{i_{1,1}, i_{1,2}, i_{1,3}, \ldots i_{1,2^{n_0-1}}\}$$
$$S_2^{n_0} = \{i_{2,1}, i_{2,2}, i_{2,3}, \ldots i_{2,2^{n_0-1}}\} \tag{17}$$

Two additional subsets of the same size are constructed using these subsets in equation (18),

$$\bar{S_1}^{n_0} = \{\{i_{1,1} + 2^{n_0}, i_{1,2} + 2^{n_0}, i_{1,3} + 2^{n_0} \ldots i_{1,2^{n_0-1}} + 2^{n_0}\}\}$$
$$\overline{S_2}^{n_0} = \{\{i_{2,1} + 2^{n_0}, i_{2,2} + 2^{n_0}, i_{2,3} + 2^{n_0} \ldots i_{2,2^{n_0-1}} + 2^{n_0}\}\} \tag{18}$$

After that, we get the subgroups with a larger size, $n = n_0 + 1$, in the following way we get equation (19),

$$S_1^{n_0+1} = S_1^{n_0} \cup \bar{S}_1^{n_0}, \qquad S_2^{n_0+1} = S_2^{n_0} \cup \bar{S}_2^{n_0} \tag{19}$$

Applying this method, one may verify that when n=5, we get equation (20),

$$S_1^5 = \{1,4,6,7,10,13,16,18,19,21,24,25,28,30,31\}$$
$$S_2^5 = \{2,3,5,8,9,12,14,15,17,20,22,23,26,27,29,32\} \tag{20}$$

So, for each user at any moment, we have $\widehat{d_{u.n}} = d_{u,n}$ *and* $i_{u,n} = 0$; these equalities hold for any number of users up to M/2. The complete data provided utilizes three characteristics of W-H codes.

2.4 Alamouti with CDMA- FBMC /OQAM

There will be some distortion in the channel, even in the most practical transmission strategy. Therefore, we will assume for the explanation that this is a perfectly synchronized wireless downlink (DL)transmission.

2.4.1 Problem Statement

It is important to note that the Alamouti decoding process replaces the channel equalization process before attempting to apply the Alamouti method to CDMA-FBMC/OQAM. The Alamouti decoding process must replace the equalization component when converting the Alamouti scheme to CDMA- FBMC/OQAM. The de spreading operation must be executed immediately after the FBMC/OQAM modulator. Next, the de spreading operation has to happen before the Alamouti decoding, which is different from the DL typical MC-CDMA scenario. In fact, the de spreading block's output is the only place where a complex orthogonality attribute may be recovered using FBMC/OQAM. The issue of whether complex orthogonality holds in CDMA-FBMC/OQAM if the de spreading operation is performed before equalization arises from this crucial point. If so, how much would it cost? The following issue arises from the first point: take into consideration the complex values t_i, β_i, λ_i.From $\sum_{i=0}^{M-1} \beta_i t_i$(despreading), is it feasible to get $\sum_{i=0}^{M-1} \beta_i t_i / \lambda_i$ (equalization + spreading)? In this case, $e_i = t_i/\lambda_i$ represents equalization, while $\sum_{i=0}^{M-1} \beta_i e_i$ represents the despreading procedure. Unless all the λ_i are equal, meaning $\lambda_i = \lambda_j = \lambda$, the response is usually (clearly) NO. This holds true in the scenario when a constant channel across frequencies is present. To be more precise, this is the only scenario in which switching the sequence of equalization and despreading processes would not negatively impact transmission quality. On the other hand, for a channel whose frequency is not constant, the performance should be affected by using despreading before equalization. Allow us to start by thinking about a flat channel. The channel co efficient will therefore affect the subset of subcarriers that have a certain spreading code applied to them.

2.5 Model Implementation

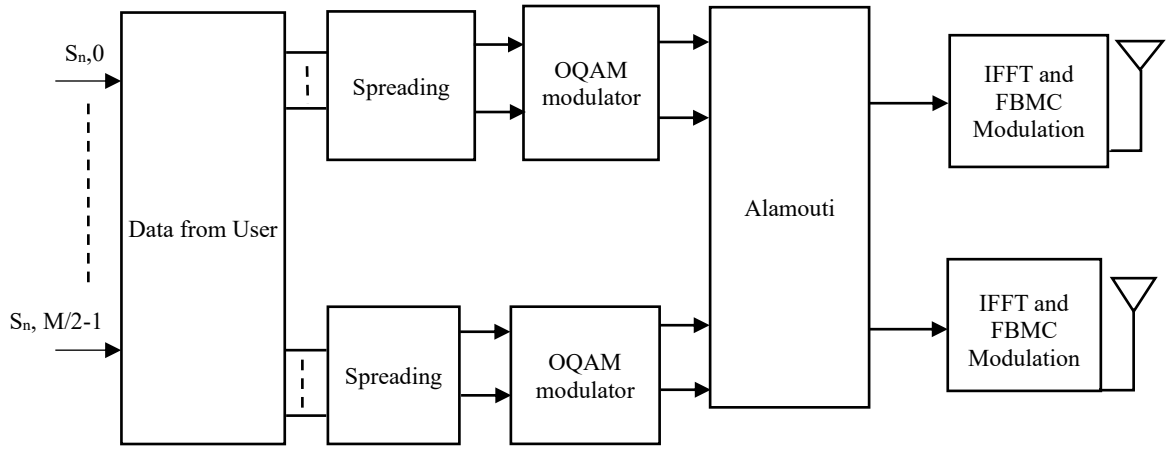

Figure 3: Alamouti CDMA- FBMC/OQAM transmitter

In order to enhance dependability of wireless communication, figure 3 demonstrates the process of transmission in a CDMA-FBMC/OQAM system coupled with Alamouti Space-Time Block Coding (STBC). The input of data to users is done first; data is entered by more than one user. Data is distributed

by use of unique codes ensuring separation of users and also increased resistance to interference. The Orthogonality and spectral efficiency of the spread signals is checked by the OQAM modulator by means of an Offset Quadrature Amplitude Modulation (OQAM). To provide diversity in the broadcast of modulated symbol pairs across two antennas, the Alamouti STBC encoding block modulated symbol pairs and after modulation, it encodes the pair of encodes into a 2 x2 space-time block matrix. To process the symbols that have been encoded, IFFT and FBMC modulation are applied. In this case, IFFT converts data in the frequency domain to the time domain signals and FBMC is used to transmit data using a multicarrier means efficiently. Lastly, the processed signals are broadcasted using two antennas, which enhances their resistance of fading and multipath effects as a result of exploiting Alamouti diversity. The combination of CDMA, FBMC and Alamouti STBC offers the improvement of signal reliability, spectrum efficiency and better interference reduction to wireless communication systems.

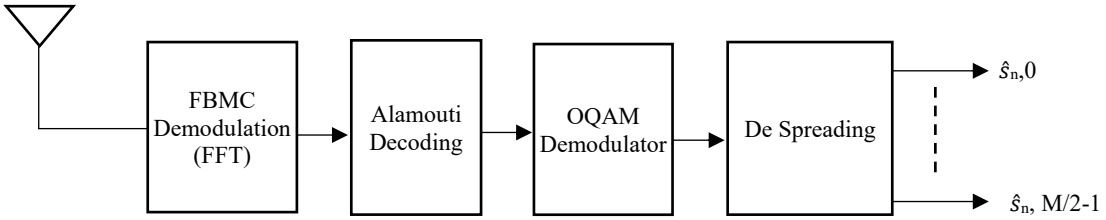

Figure 4: CDMA- FBMC/OQAM receiver of Alamouti

Figure 4 demonstrates a CDMA-FBMC/OQAM transmission system with Alamouti Space-Time Block Coding (STBC), and the receiver structure has a flow diagram. The delivered data should initially be processed by the receiver through some series of operations referred to as signal extraction. The FBMC demodulation process is the first step and its FFT-based processing is applied on the received signal. In this case, the recovered subcarriers are obtained with the help of Fast Fourier Transform (FFT) and Polyphase filter bank (PPN) and spectral efficiency is preserved. The Alamouti decoding block receives the demodulated signal and applies space-time diversity algorithm in restoring the original broadcast symbols in the two received signals. This helps in the strength of the signal and minimizes the effects of channel fading. To recover the originally reflected symbols, OQAM demodulation of the signal is done following the Alamouti decoding. This is a process of individually processing and adding the real and imaginary elements of the signal and synchronizing them. Then there is the de-spreading procedure, which is effective in the reduction of multi-user interference by making use of user-specific spreading codes (applied at the transmitter) to isolate data of individual users. Finally, the symbols that were reconstructed (which are displayed as ŝn,0 to ŝn, M/2-1) represent the reconstructed information in many users. The receiver architecture is developed in such a way that it enhances reliability, spectrum efficiency, resistance to interference and fading so that it can be used in a multi-user communication.

At multiple-input multiple-output (MIMO) instant n, the de spread signal is as in equation (21):

$$z^{c}_{n_0,u_0} = h_{n_0,i} d^{c}_{n_0,u_0,i} \tag{21}$$

At time instant n0, the complex data of the user u 0, denoted by $d^{c}_{n_0,u_0,i}$, is being sent by antenna i.

Here we have a system with two antennas, each with an index of 0 and 1, and we apply the Alamouti coding scheme to the data of each user u, where $s_{k,u}$ is the user u main stream of complex data, we can get equation (22),

$$d^{c}_{2k,u,0} = \frac{s_{2k,u}}{\sqrt{2}}$$

$$d^{c}_{2k,u,1} = \frac{s_{2k+1,u}}{\sqrt{2}} \tag{22}$$

At time $2k+1$, we can get equation (23),

$$d^{c}_{2k,u,0} = \frac{-\left(s_{2k+1,u}\right)^{*}}{\sqrt{2}}$$

$$d^{c}_{2k+1,u,1} = \frac{s^{*}_{2k}}{\sqrt{2}} \tag{23}$$

Bypassing noise, the de spreading signal for user u on a flat fading channel is

$$z^{c}_{n,u} = h_{n,0} d^{c}_{n,u,o} + h_{n,1} d^{c}_{n,u,1}$$

Then,

$$\begin{bmatrix} z^{c}_{2k,u} \\ {z^{c}_{2k+1,u}}^{*} \end{bmatrix} = \underbrace{\frac{1}{\sqrt{2}} \begin{bmatrix} h_{2k,0} & h_{2k,1} \\ \left(h_{2k+1,1}\right)^{*} & -\left(h_{2k+1,0}\right)^{*} \end{bmatrix}} \begin{bmatrix} s_{2k,u} \\ s_{2k+1.u} \end{bmatrix} \tag{24}$$

The decoding equation given in Section 2.2 is identical to the one used in the Alamouti technique. Therefore, the decoding might also be done in the same manner. Figure 3 shows the Alamouti CDMA-FBMC/OQAM transmitter, while figure 4 shows the Alamouti receiver.

3 Simulation Results

This section assesses the suggested FBMC-OQAM's performance in a MIMO setting. The proposed model was implemented and validated using the MATLAB 2022a platform. Its performance was assessed by computing BER, PSD, PAPR, and ISI under varying channel conditions. In addition to this, results were compared with benchmark models to validate the proposed approach.

3.1 Bit Error Rate Analysis

In order to determine the efficacy of the suggested model in terms of data samples fit, the performance is fully checked by comparing BER with SNR. Specifically, the spreading in time domain of Walsh-Hadamard is used to repair the complex orthogonality of the FBMC-OQAM system. This is essential because Alamouti coding is based on the fact that there is complex orthogonality in the process of transmission. Moreover, every code within system is also orthogonal to itself even with the delay factor, thereby gives an extra strength against other possible problems, like Inter-Symbol Interference (ISI) (Xu et al., 2021).

Table 1: Simulation parameters of the proposed model

Parameters	Value
Spreading length	8
Modulation order	16
SNR	0 to 30dB
Number of symbols	30
Overlapping factor	4
Channels	AWGN, Pedestrian A, Vehicular A
MIMO	2X1,2X2 with ZF, 2x2 with ML

This orthogonality guarantees that the system is able to manage the signal degradation caused by ISI which is one of the major problems in wireless communications. The analytical validation of the system

of proposed model efficiency is realized through the detailed analysis of performance on the basis of BER. This analysis is done with respect to MIMO-FBMC-OQAM which uses CDMA with Alamouti space-time coding, ZF and Maximum Likelihood (ML) detection. They are tried in different channel conditions such as pedestrian A channels, and Vehicular A channels. Table 1 displays simulation parameters that were applied in this evaluation.

3.2 Performance Comparison on Various Channels

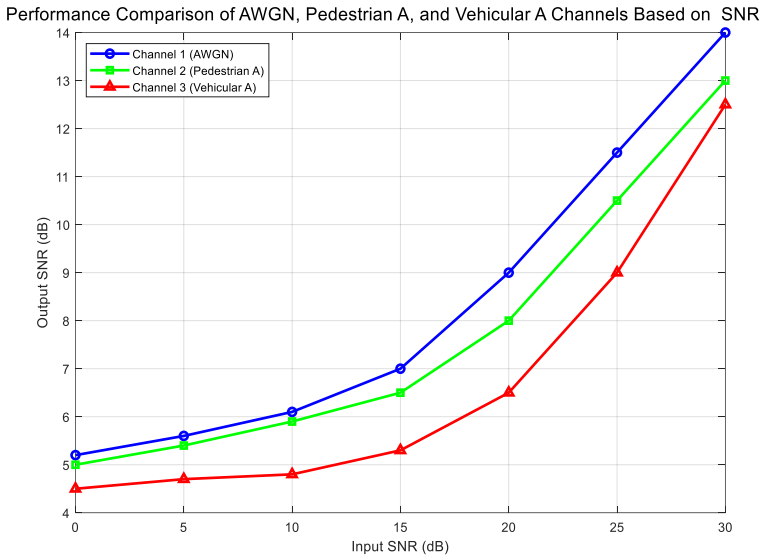

Figure 5 (a): Performance comparison of AWGN, pedestrian A, and vehicular a channels based on input SNR vs output SNR

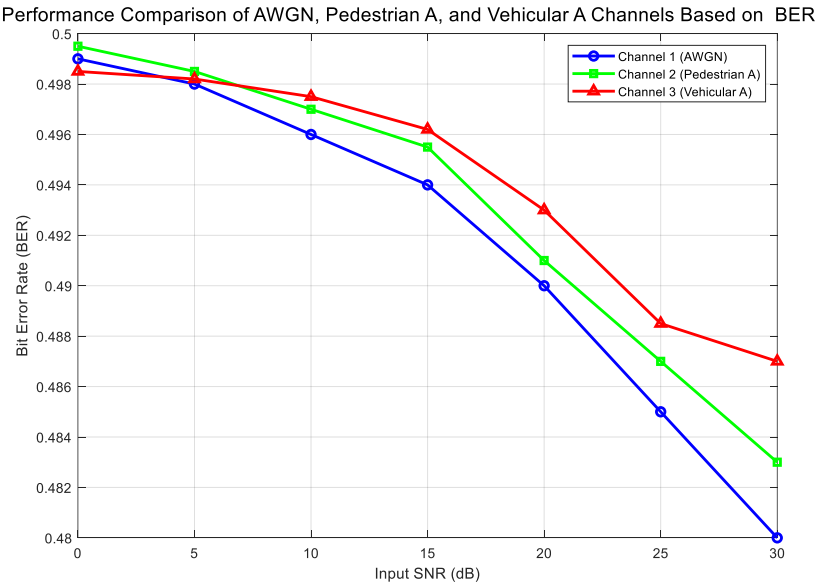

Figure 5 (b): Performance comparison of AWGN, pedestrian A, and vehicular a channels based on output BER

Figure 5 (a, b) shows the behaviour of three wireless communication channels (AWGN, Pedestrian A, and Vehicular A -) at different SNR, where the outcome SNR and BER are taken into consideration in the context of a 32-subcarrier system. The AWGN channel represented by blue has the largest output SNR, and the lowest BER of all input SNR, and is the theoretically best environment based on the absence of multipath or fading effects. The Pedestrian A channel, which is shown in green, has slightly poorer performance, and both the output SNR and the BER is moderately degraded by the low-mobility fading nature, which is very slow. The Vehicular A channel, illustrated in the red colour, exhibits the lowest SNR output and the highest BER, which represents the problems of high mobility fast fading and Doppler spread. In general, the graph indicates clearly that AWGN is better performing, and the fading effects found in Pedestrian A and Vehicular A diminish the efficiency of the system especially when it comes to the error rate and signal quality when SNR attains higher values.

Figure 6(a), (b), (c) is a comparative study of the Signal to Interference plus Noise Ratio (SINR) performance of the Standard and Optimized FBMC-CDMA systems in three subcarrier configurations namely; 32, 64 and 128. The sub plots show how SINR changes with the SNR values of 1dB to 7 dB and the number of transmit antennas (N t = 1, 2, 4). The optimized FBMC-CDMA system in subplot (a) shows the optimized SNR of all the SNR levels and all the antenna configurations better than the standard model had 32 subcarriers. It is important to note that the optimized system, N t = 4 has the largest SINR with maximum of 16 dB at SNR = 7dB which means that it has a very good interference suppression. The same tendency can be noticed once we shift to subplot (b), where the number of subcarriers is 64; the values of the optimized system are somewhat lower than the ones of the standard system on average, but still, the optimized system is better than the standard one. The profitability is more evident at high SNR, and the optimized model exhibits more steep increase in SINR. Subplot (c) which depicts 128 subcarriers, the SINR is also slightly reduced in all the configurations because the spectral division is more refined, and prone to being affected by interference. Nevertheless, in this denser spectral environment optimised FBMC-CDMA system still has better performance and particularly when Nt is higher; it has reached SINR values near to 13.5 dB. One can find that the optimized FBMC-CDMA system is always able to provide a better SINR in all three subcarrier settings, and the higher the number of transmit antennas is, the higher the optimized SINR. This shows the effectiveness and strength of the optimized model in avoidance of the interference and the improvement of the signal quality within multi-carrier communication systems.

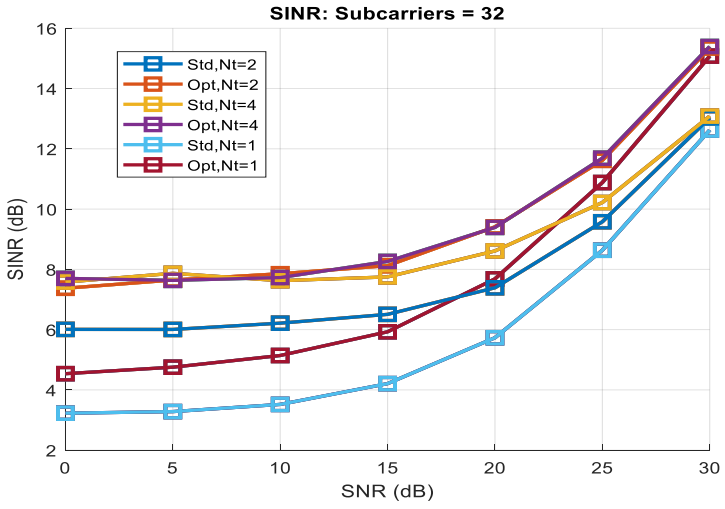

(a)

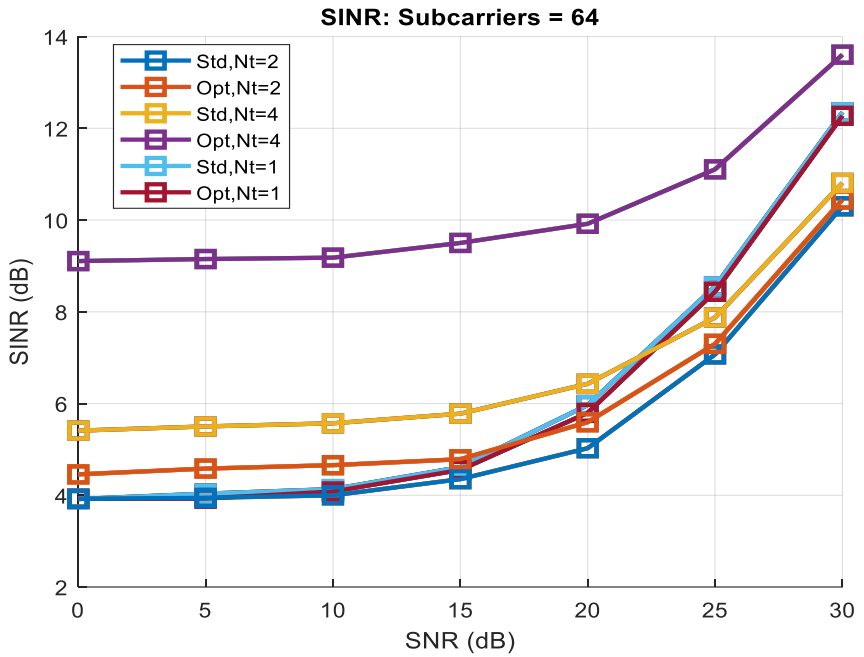

(b)

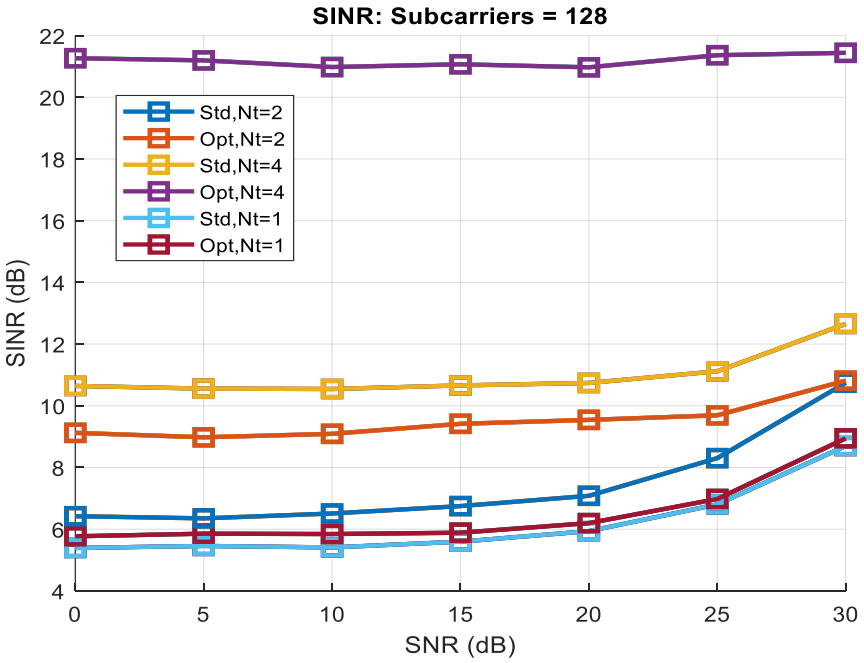

(c)

Figure 6: Comparative analysis of proposed model regarding SINR Vs SNR of different subcarriers (a) 32 subcarriers, (b) 64 subcarriers and (c)128 subcarriers

Figure 7(a), (b), (c) illustrates a comparative study of the Bit Error Rate (BER) performance of the standard and optimized FBMC-CDMA models stated under different conditions of subcarriers (32, 64 and 128) and transmit antenna configurations (N t = 1, 2 and 4). Every subplot is a representation of the

number of subcarriers and measures the variation of BER with the Signal-to-Noise Ratio (SNR) increase between 1 dB and 30 d B. Regarding subplot (a), or 32 subcarriers, we can see that the optimized FBMC-CDMA model is always superior compared to the standard model in all the antenna configurations. In particular, the model optimized with increasing the number of transmit antennas shows increased reduction in BER, and the model shows the best performance with N t = 4, which shows BER having a value of below 0.46 at 7 dB SNR. The plot (b) illustrating the case with 64 subcarriers reveals the same trend but with slightly lower gains as in the case of 32 subcarriers. The optimized model remains to have lower BER at all the SNR levels but with more differentiation as the number of antennas increases. The subplot (c) which is the 128 subcarriers shows that both models have a slight negative change in the performance of BER with an increase in the number of subcarriers, probably because of the inter-symbol interference and complexity. Nevertheless, the optimized FBMC-CDMA model continues to perform much better with respect to BER performance as opposed to the normal counterpart, especially in cases where N t = 4 where BER reduces very steeply with increasing SNR after 5 d B. All in all, these plots demonstrate that the optimized model has the benefit of reducing the number of errors and that performance is enhanced more with increased SNRs and the number of transmit antennas. Systems where the subcarrier density of the performance is large are especially critical since the optimized model is more resilient to errors over a more complicated spectral environment.

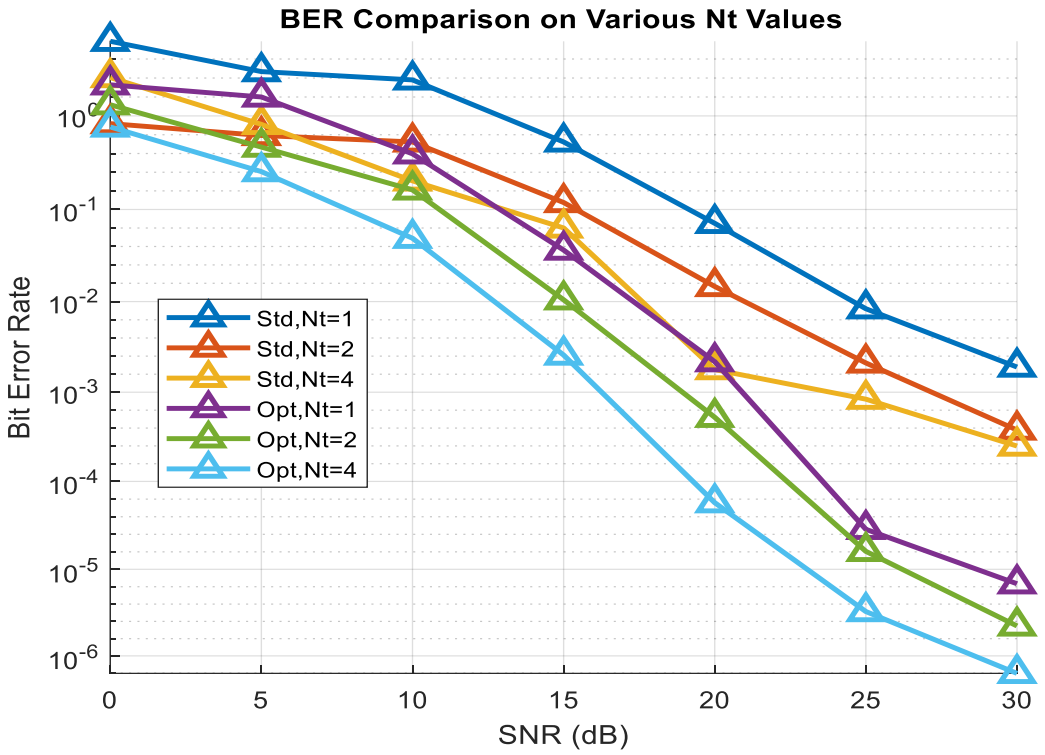

(a)

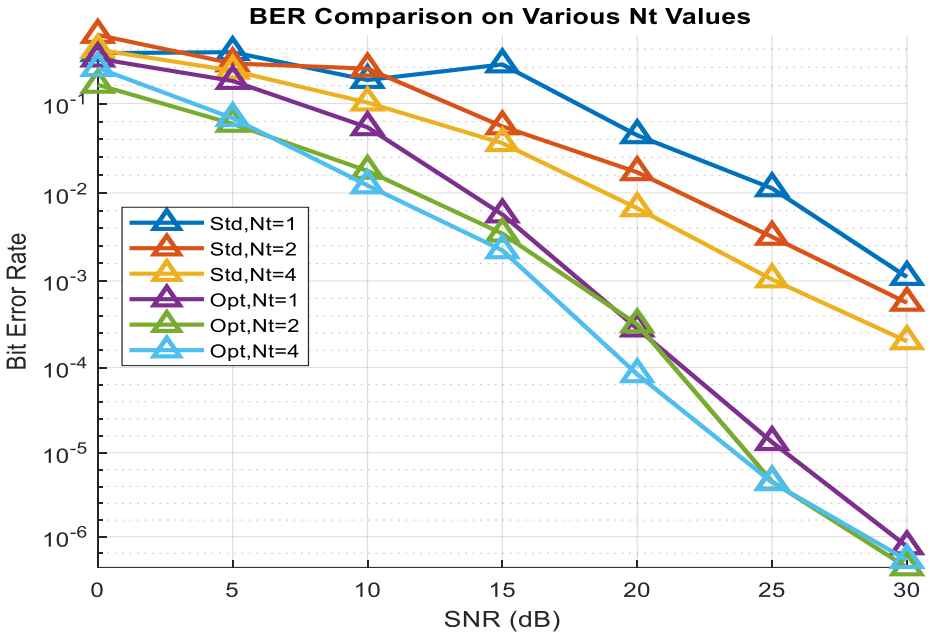

(b)

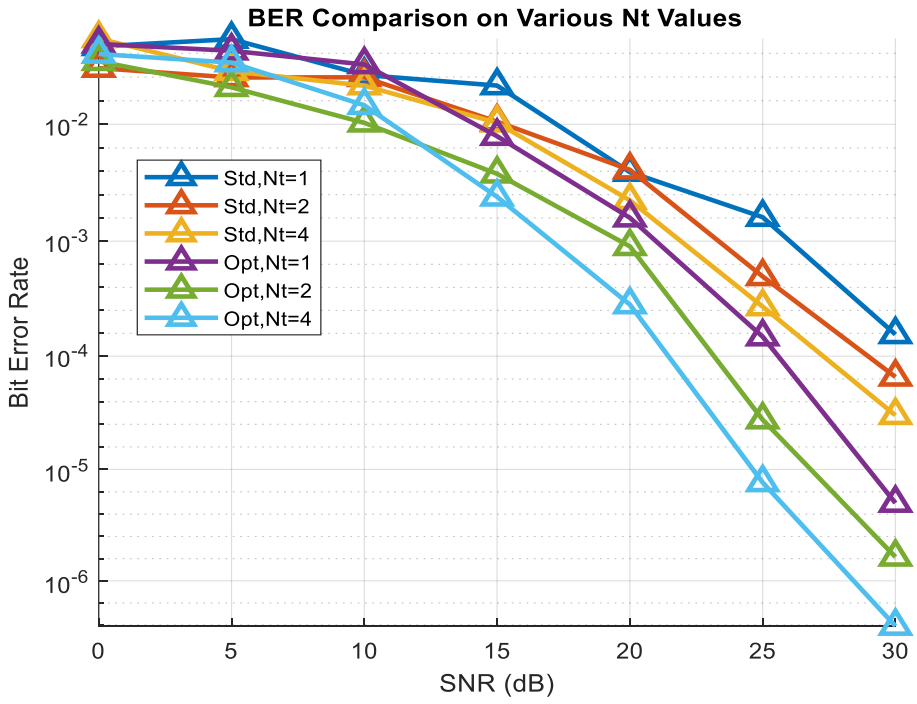

(C)

Figure 7: BER performance comparison on various subcarriers (a) 32 subcarriers, (b) 64 subcarriers, and (c) 128 subcarriers

3.2 Power Spectral Density Analysis

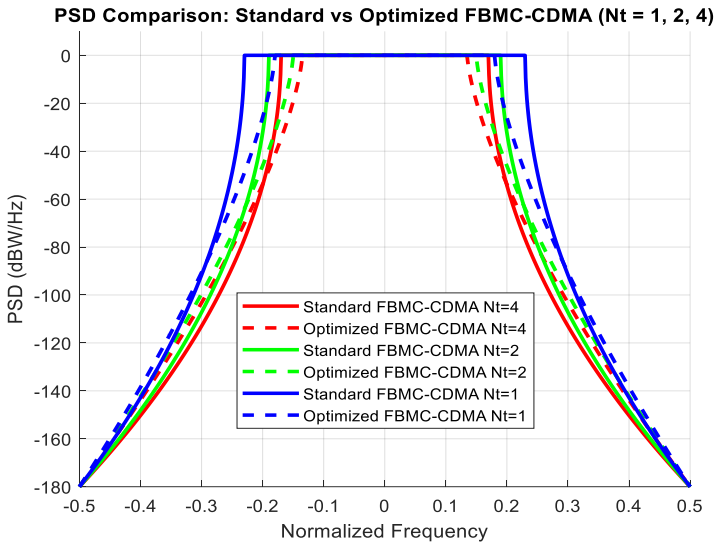

Figure 8: PSD of the proposed method and earlier models

The Power Spectral Density (PSD) presented in figure 8 illustrates the spectral behavior of standard and optimized FBMC-CDMA systems across varying transmit antenna configurations (N t = 1, 2, and 4). The horizontal axis is the normalized frequency and that of the vertical axis is the PSD in dB W/Hz. Based on the plot, it can be seen that the optimized FBMC-CDMA configurations (that are represented by the dashed lines) have better spectral containment than their standard counterparts (that are represented by the solid lines) at the side lobes. This implies that there is a very big lowering of out-of-band (OOB) emissions and this is essential in minimizing adjacent channel interference. Moreover, the sharpening of the edges and a flatter passband of the PSD curves which increases with the number of transmit antennas show the improvement of spectral efficiency. It is important to note that the FBMC-CDMA system that has been optimized to use N t = 4 displays the narrowest spectral properties and the optimization has been effective in providing spectral shaping and mitigating spectral leakage.

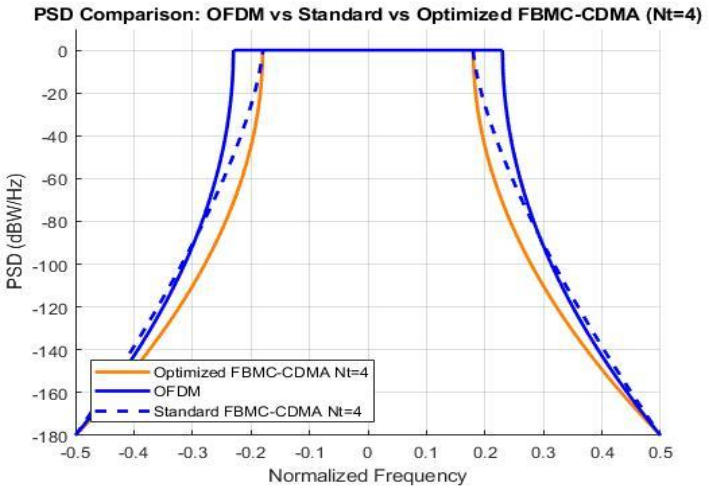

Figure 9: PSD of the proposed method over standard and optimized

Figure 9 shows that the optimized FBMC-CDMA system exhibits significantly lower out-of-band emissions, indicating better spectral containment and reduced interference. The Standard FBMC-CDMA (blue dashed line) shows moderate spectral leakage. In contrast, OFDM (blue solid line) exhibits the highest sidelobe energy, implying more spectral leakage and poor frequency localization. This indicates how optimization works in FBMC-CDMA in enhancing spectral efficiency and reducing adjacent channel interference.

3.3 Performance Comparison

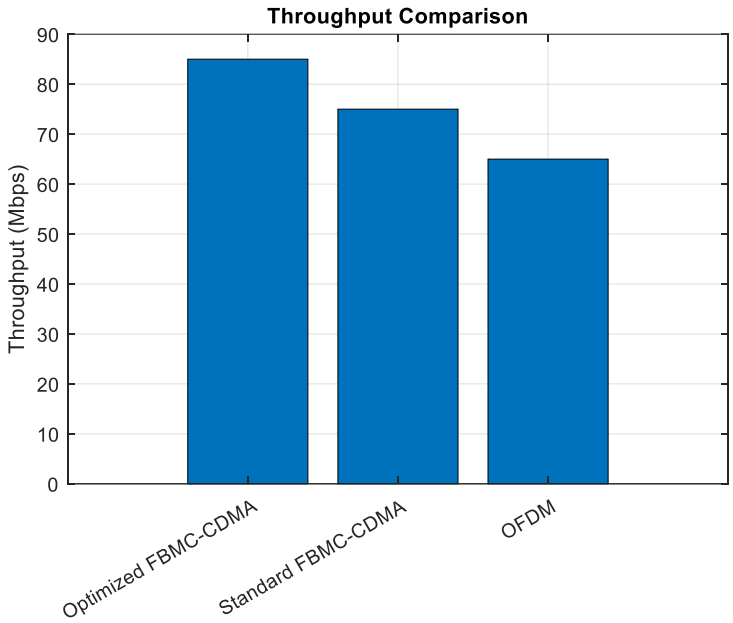

Figure 10: Performance comparison of throughput with the previous model

In figure 10, the three communication methods, Optimized FBMC-CDMA, Standard FBMC-CDMA and OFDM have been compared in terms of throughput in Mbps. The throughput is shown in Megabits per second (Mbps) in the y-axis and the various techniques in the x-axis. In the chart, it is clear that Optimized FBMC-CDMA is the one that has the maximum throughput, then Standard FBMC-CDMA, and the next one, which has the lowest throughput, is the OFDM. In particular, Optimized FBMC-CDMA attains a speed of about 85 Mbps, Standard FBMC-CDMA at about 75 Mbps and the throughput of the OFDM at about 65 Mbps.

Figure 11 shows the comparison between the Peak-to-Average Power Ratio (PAPR) of Optimized FBMC-CDMA, Standard FBMC-CDMA and that of OFDM in decibels (dB). The y-axis is used to indicate the PAPR in dB, and the x-axis is used to indicate the respective communication techniques. As can be observed in the chart, Optimized FBMC-CDMA has the lowest PAPR which is about 6.5 d B. The PAPR of Standard FBMC-CDMA is higher with 8.2 dB whereas the highest PAPR between the three is that of the OFDM with 10.5 db. Lower PAPR is generally desirable in communication systems as it reduces the requirements for the power amplifier's dynamic range and improves power efficiency.

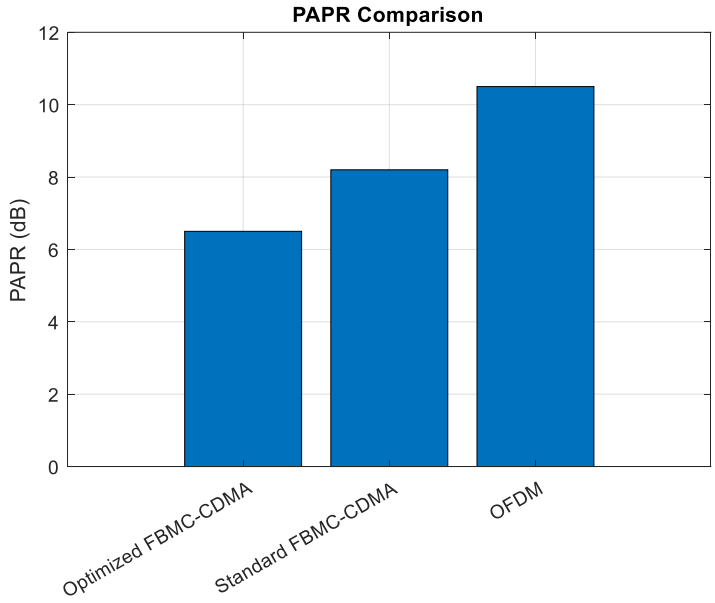

Figure 11: Performance comparison of PAPR with the previous model

4 Conclusion

The current paper has proposed a low-complexity FBMC-OQAM system incorporating CDMA and space-time coding in a Multiple-Input Multiple-Output (MIMO) system. The proposed system greatly improved performance as it has been used to provide a spreading technique to the data symbols that assist in restoring complex orthogonality property of the system. Using this model, the spreading method of FBMC-OQAM makes it possible to easily utilize other methods of MIMO, such as CDMA and space-time coding in the MIMO-FBMC-OQAM architecture. The suitable coding matrix was derived and put into place to guarantee orthogonality of FBMC-OQAM.

The suggested model has been thoroughly tested, and its efficiency has been compared to some of the previous approaches to the subject. Further, the performance of the methodology was evaluated in three configurations of different MIMO systems namely 1 x 1, 2 x 1 and 4 x 1, using varying values of transmit antennas while maintaining a fixed receive antenna. The standard and optimized strategies were compared based on BER. The comparative analysis revealed that the proposed approach worked better than existing models in almost every situation and possesses a higher performance and efficiency. The findings support the possibilities of the low-complexity FBMC-OQAM system as an effective solution to the modern MIMO communication systems.

References

[1] Abdel-Atty, H. M., Raslan, W. A., & Khalil, A. T. (2020). Evaluation and analysis of FBMC/OQAM systems based on pulse shaping filters. *IEEE Access*, *8*, 55750-55772. https://doi.org/10.1109/ACCESS.2020.2981744

[2] Alamouti, S. M. (2002). A simple transmit diversity technique for wireless communications. *IEEE Journal on selected areas in communications*, *16*(8), 1451-1458. https://doi.org/10.1109/49.730453

[3] Arjun, R., Shah, H., Dhua, S., Appaiah, K., & Gadre, V. M. (2021). Low complexity FBMC for wireless MIMO systems. *Physical Communication*, *47*, 101332. https://doi.org/10.1016/j.phycom.2021.101332

[4] Bedoui, A., & Et-tolba, M. (2021). A deep neural network-based interference mitigation for MIMO-FBMC/OQAM systems. *Frontiers in Communications and Networks*, *2*, 728982. https://doi.org/10.3389/frcmn.2021.728982

[5] Caus, M., & Perez-Neira, A. I. (2013). Multi-stream transmission for highly frequency selective channels in MIMO-FBMC/OQAM systems. *IEEE transactions on signal processing*, *62*(4), 786-796. https://doi.org/10.1109/TSP.2013.2293973

[6] Chen, D., Tian, Y., Qu, D., & Jiang, T. (2018). OQAM-OFDM for wireless communications in future Internet of Things: A survey on key technologies and challenges. *IEEE Internet of Things Journal*, *5*(5), 3788-3809. https://doi.org/10.1109/JIOT.2018.2869677

[7] ChithraDevi, S. A., Mahendravarman, I., Ragavendiran, A., Selvam, M. M., Yamuna, K., & Vibin, R. (2024, July). Optimal configuration of radial distribution networks with stud krill herd optimization. In *2024 International Conference on Signal Processing, Computation, Electronics, Power and Telecommunication (IConSCEPT)* (pp. 1-6). IEEE. https://doi.org/10.1109/IConSCEPT61884.2024.10627797

[8] De Almeida, I. B. F., Mendes, L. L., Rodrigues, J. J., & Da Cruz, M. A. (2019). 5G waveforms for IoT applications. *IEEE Communications Surveys & Tutorials*, *21*(3), 2554-2567. https://doi.org/10.1109/COMST.2019.2910817

[9] Dinan, E. H., & Jabbari, B. (2002). Spreading codes for direct sequence CDMA and wideband CDMA cellular networks. *IEEE communications magazine*, *36*(9), 48-54. https://doi.org/10.1109/35.714616

[10] Ghazi, A., Aljunid, S. A., Idrus, S. Z. S., Fareed, A., Al-dawoodi, A., & Mohsin, A. H. (2021, February). Design of a hybrid WDMA-Optical-CDMA over multi-mode fiber transmission system based on LG modes for short haul-local area network. In *Journal of Physics: Conference Series* (Vol. 1793, No. 1, p. 012016). IOP Publishing. https://doi.org/10.1088/1742-6596/1793/1/012016

[11] Kadhim, A. A., Mohammed, S. J., & Al-Gayem, Q. (2024). DVB-T2 Energy and Spectral Efficiency Trade-off Optimization based on Genetic Algorithm. *Journal of Internet Services and Information Security, 14*(3), 213-225. https://doi.org/10.58346/JISIS.2024.I3.012.

[12] Le, C., Moghaddamnia, S., & Peissig, J. (2016, August). On the performance of Alamouti scheme in 2 x 2 MIMO-FBMC systems. In *ICOF 2016; 19th International Conference on OFDM and Frequency Domain Techniques* (pp. 1-6). VDE.

[13] Lélé, C., Siohan, P., & Legouable, R. (2010). The alamouti scheme with CDMA-OFDM/OQAM. *EURASIP Journal on Advances in Signal Processing*, *2010*(1), 703513. https://doi.org/10.1155/2010/703513

[14] Lélé, C., Siohan, P., Legouable, R., & Bellanger, M. (2007). CDMA transmission with complex OFDM/OQAM. *EURASIP Journal on Wireless Communications and Networking*, *2008*(1), 748063. https://doi.org/10.1155/2008/748063

[15] Lélé, C., Siohan, P., Legouable, R., & Bellanger, M. (2007, May). OFDM/OQAM for Spread-Spectrum Transmission. In *Multi-Carrier Spread Spectrum 2007: Proceedings from the 6th International Workshop on Multi-Carrier Spread Spectrum, May 2007, Herrsching, Germany* (pp. 157-166). Dordrecht: Springer Netherlands.

[16] Lenine, D., Kumar, P. S. S., Reddy, B. V., Jagadeesh, K., Kiran, P. S., & Kumari, J. S. (2025). An Adaptive MPC for Alternate Arm Modular Multilevel Converter PV Tied Grid Connected HVDC Transmission Network. *Archives for Technical Sciences*, *2*(33), 442-452. https://doi.org/10.70102/afts.2025.1833.442

[17] Li, J., Li, S., Dong, H., & Li, Z. (2022). Intrinsic interference cancellation scheme for FBMC-OQAM systems based on power multiplexing. *Electronics*, *11*(9), 1443. https://doi.org/10.3390/electronics11091443

[18] Nissel, R., Schwarz, S., & Rupp, M. (2017). Filter bank multicarrier modulation schemes for future mobile communications. *IEEE Journal on Selected Areas in Communications*, *35*(8), 1768-1782. https://doi.org/10.1109/JSAC.2017.2710022

[19] Perez-Neira, A. I., Caus, M., Zakaria, R., Le Ruyet, D., Kofidis, E., Haardt, M., ... & Cheng, Y. (2016). MIMO signal processing in offset-QAM based filter bank multicarrier systems. *IEEE Transactions on Signal Processing*, *64*(21), 5733-5762. https://doi.org/10.1109/TSP.2016.2580535

[20] Popovski, P., Trillingsgaard, K. F., Simeone, O., & Durisi, G. (2018). 5G wireless network slicing for eMBB, URLLC, and mMTC: A communication-theoretic view. *Ieee Access*, *6*, 55765-55779. https://doi.org/10.1109/ACCESS.2018.2872781

[21] Raslan, W. A., Mohamed, M. A. A., & Abdel-Atty, H. M. (2022). Efficient Implementation of MIMO FBMC/OQAM Scheme based on Block Spreading. *Delta University Scientific Journal*, *5*(1), 66. https://doi.org/10.21608/dusj.2022.233923

[22] Renfors, M., Mestre, X., Kofidis, E., & Bader, F. (Eds.). (2017). *Orthogonal waveforms and filter banks for future communication systems*. Academic Press.

[23] RezazadehReyhani, A., & Farhang-Boroujeny, B. (2017). Capacity analysis of FBMC-OQAM systems. *IEEE Communications Letters*, *21*(5), 999-1002.

[24] Sahin, A., Guvenc, I., & Arslan, H. (2013). A survey on multicarrier communications: Prototype filters, lattice structures, and implementation aspects. *IEEE communications surveys & tutorials*, *16*(3), 1312-1338. https://doi.org/10.1109/SURV.2013.121213.00263

[25] Säily, M., Estevan, C. B., Gimenez, J. J., Tesema, F., Guo, W., Gomez-Barquero, D., & Mi, D. (2020). 5G radio access network architecture for terrestrial broadcast services. *IEEE Transactions on broadcasting*, *66*(2), 404-415. https://doi.org/10.1109/TBC.2020.2985906

[26] Şimşir, Ş. (2024). An advanced symbol detection approach for MIMO-FBMC/OQAM scheme based on migrating birds optimization algorithm. *EURASIP Journal on Wireless Communications and Networking*, *2024*(1), 80. https://doi.org/10.1186/s13638-024-02410-3

[27] Singh, P., Budhiraja, R., & Vasudevan, K. (2018). SER analysis of MMSE combining for MIMO FBMC-OQAM systems with imperfect CSI. *IEEE Communications Letters*, *23*(2), 226-229. https://doi.org/10.1109/LCOMM.2018.2884932

[28] Tandon, B., & Thakur, M. (2025). An Overview of Adaptive Signal Processing Methods for 6G Wireless Communication Networks. *International Academic Journal of Science and Engineering*, *12*(1), 12–15. https://doi.org/10.71086/IAJSE/V12I1/IAJSE1203

[29] Tse, D., & Viswanath, P. (2005). *Fundamentals of wireless communication*. Cambridge university press.

[30] Varlamov, V. O., Lobov, E. M., & Lobova, E. O. (2023). Investigation of FBMC-OQAM equalization with real interference prediction algorithm properties for MIMO transmission scheme. *Sensors*, *23*(4), 2111. https://doi.org/10.3390/s23042111

[31] Walia, A., Rai, D. S., Kataria, A., Hota, S., Kamalashekaran, J., & Saisindhutheja, R. (2025). Edge-aware routing protocols for low-latency Internet services. *Journal of Internet Services and Information Security*, *15*(3). https://doi.org/10.58346/JISIS.2025.I3.038

[32] Wang, H., Xu, L., Wang, X., & Taheri, S. (2018). Preamble design with interference cancellation for channel estimation in MIMO-FBMC/OQAM systems. *IEEE Access*, *6*, 44072-44081. https://doi.org/10.1109/ACCESS.2018.2864221.

[33] Wang, S., Zhu, S., & Zhang, G. (2010). A Walsh-Hadamard coded spectral efficient full frequency diversity OFDM system. *IEEE transactions on communications*, *58*(1), 28-34. https://doi.org/10.1109/TCOMM.2010.01.070605

[34] Xu, Y., Feng, Z., Zou, J., Kong, D., Xin, Y., & Jiang, T. (2021). An imaginary interference-free method for MIMO precoding in FBMC/OQAM systems. *IEEE Transactions on Broadcasting*, *67*(3), 642-650. https://doi.org/10.1109/TBC.2021.3051528

[35] Zakaria, R., & Le Ruyet, D. (2012). A novel filter-bank multicarrier scheme to mitigate the intrinsic interference: Application to MIMO systems. *IEEE Transactions on Wireless Communications*, *11*(3), 1112-1123. https://doi.org/10.1109/TWC.2012.012412.110607

Authors Biography

Satish Kanapala received Bachelor's degree in Electronics and Communication Engineering from Jawaharlal Nehru Technological University (JNTU), Hyderabad, India, in 2007, and Master's degree with specialization Communication Systems from JNTU Hyderabad in 2010. His research interests include digital communication system, wireless communication, multicarrier modulation, signal processing for 5G and beyond.

Shaik Jakeer Husain received his B.E. degree in Electronics and Communication Engineering from Andhra University, Visakhapatnam in 1996, and M.E. degree in Digital System from Osmania University, Hyderabad in 2008. He received his Ph.D. in Digital Signal Processing from JNTU, Hyderabad in 2016.He is currently a Professor in Department of Electronics and Communication Engineering at Vignan's Foundation for Science, Technology and research, Guntur. His research interests include Biomedical Signal Processing, Digital Signal Processing and Machine Learning.